Movement analysis of normal and pathological gait

Michael Voigt Ph.D.

Center for Sensory-Motor Interaction (SMI)
Dept. of Health Science and Technology
Aalborg University
Denmark

Content

- Acquisition of kinematic and kinetic information
- Sources of error
- Combining kinematic and kinetic information
- Inverse dynamic calculations
- Examples
- Extending inverse dynamic analysis of human movement to muscle forces

Kinematic information

Eadweard Muybridge (1830 – 1904)

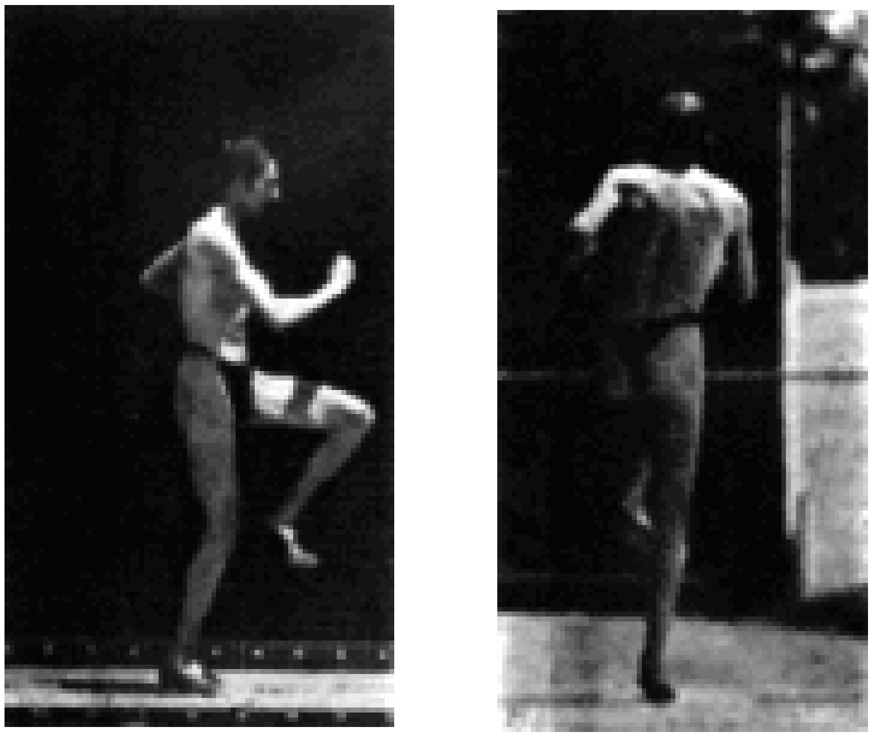

- Kinematics of human performance (one legged jump)

Video technology
– with reflective markers and (semi-)automatic detection

1. Reflective markers are mounted on the target object.
2. The camera emits infrared (IR) flashes from IR-diodes synchronized with the camera shutter.
3. In each ‘picture frame’ the camera records the reflected IR-light from the markers over a period determined by the shutter speed.
4. The picture information is lost and only the bright spots corresponding to reflected light from the markers are ‘seen’ by the cameras.
5. The video pictures are digitized.
6. The firmware in the cameras identifies the bright pixel clusters corresponding to the marker reflections and calculates the x-y coordinates of the centroid.
7. The 2D camera coordinates are sent to a PC through a high speed serial connection. For further processing and calibration

- ProReflex cameras (1 – 1000 frs s^{-1})

http://www.qualisys.se

<u>Other manufacturers:</u>

Vicon ™ (http://www.oxfordmetrics.com)

Motion Analysis™ Corp. (http://motionanalysis.com)

Elite™ (http://www.bts.it)

Peak Performance Technologies™ (http://www.peakperform.com)

Etc.

Determination of marker positions in 3D - direct linear transformation

- A calibration of N points with known coordinates x_r, y_r, z_r (r = 1,….,N) is used for determination of coefficients a_{kj} for each camera
- 11 coefficients have to be determined
- each camera is described by two equations
- as long as a minimum of two cameras are used 6 calibration points gives 12 equations
- the over-determined of system of linear equations is solved by least squares technique

- the solution is not unique since the measurements are not perfect and the solution is approximated by minimizing errors (Δ_j) i.e. the 'norm of residuals' (NR) defined as:

$$NR = \sqrt{\Delta_1^2 + \Delta_2^2 + \ldots + \Delta_n^2}$$

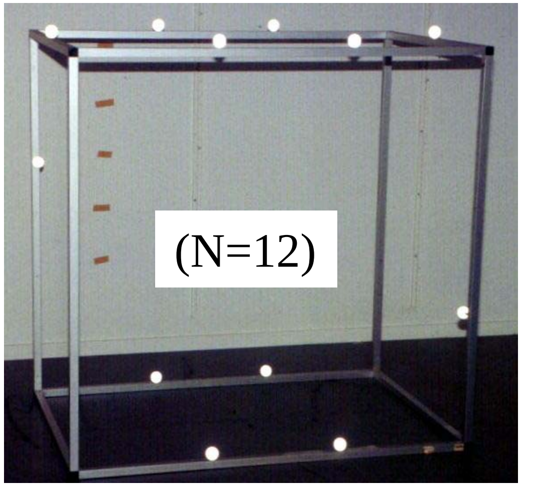

Determination of marker positions in 3D – technical issues of accuracy

- Accuracy of the calibration frame
- Quality of the DLT (Direct Linear Transformation) reconstruction
- Quality of the lenses
- Resolution of the light sensitive chip

Kinematics of human movement
– recorded with reflective markers

- reflective markers are positioned on the body depending on the aim (2D or 3D)
- the marker positions are recorded

From the positions of the markers i derived :
- the coordinates of the segment endpoints
- segment angles and derivatives
- joint angles and derivatives
- segment lengths

Combined with the anthropometric information the following is obtained:
- positions of the center of masses of the segments

Embedded coordinate systems

- 3D reconstruction of body segment coordinate systems from markers

- using minimum three markers pr segment to describe 6 DOF

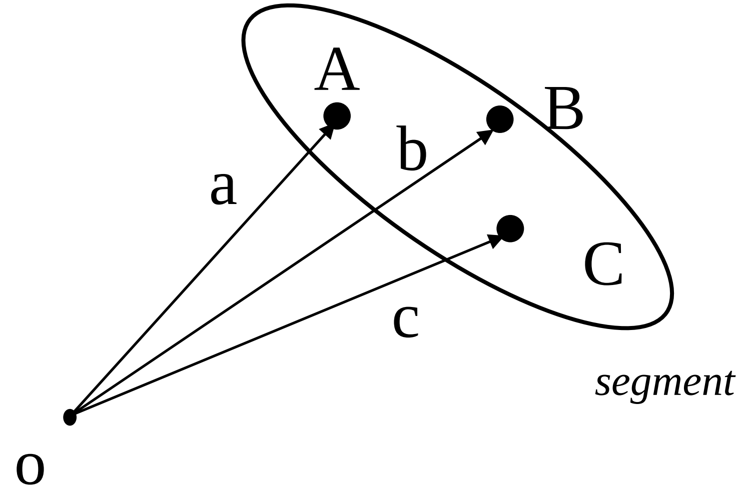

$$\xi'\mathbf{1} = \frac{\mathbf{b}-\mathbf{a}}{|\mathbf{b}-\mathbf{a}|}$$

$$\xi'\mathbf{3} = \xi'\mathbf{1} \times \frac{\mathbf{c}-\mathbf{a}}{|\mathbf{c}-\mathbf{a}|}$$

$$\xi'\mathbf{2} = \xi'\mathbf{3} \times \xi'\mathbf{1}$$

A = first marker on the segment of interest
B = second marker on the segment of interest
C = third marker on the segment of interest
a = position vector of point A in the lab coordinate system
b = position vector of point B in the lab coordinate system
c = position vector of point C in the lab coordinate system
$\xi'\mathbf{1}$ = direction vector of the first axis of the segment coordinate system
$\xi'\mathbf{2}$ = direction vector of the second axis of the segment coordinate system
$\xi'\mathbf{3}$ = direction vector of the third axis of the segment coordinate system

Errors in motion of ‘rigid’ ¨body segments
- using skin mounted markers

- marker movement (skin mounted markers)
  - errors due to relative marker movement

    (movement of markers in relative to each other)

    - can be solved by using marker attachment systems/frames

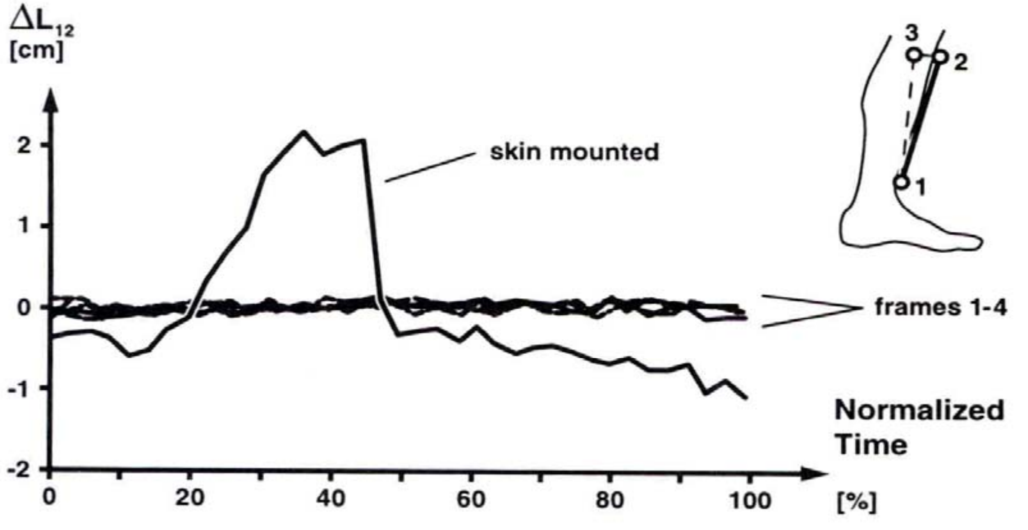

Figure 3.6.7 Actual three-dimensional length between the markers 1 and 2 during ground contact in running (time 0 corresponds to heel strike, time 100% to take-off) for four marker frames and for skin-mounted markers. The graph illustrates results for one subject and is representative of the general trend (from Ronsky and Nigg, 1993, with permission).

Errors in motion of 'rigid' body segments – deriving joint angles in 3D

- knee joint kinematics with bone mounted markers
  - four coordinate transformations are involved

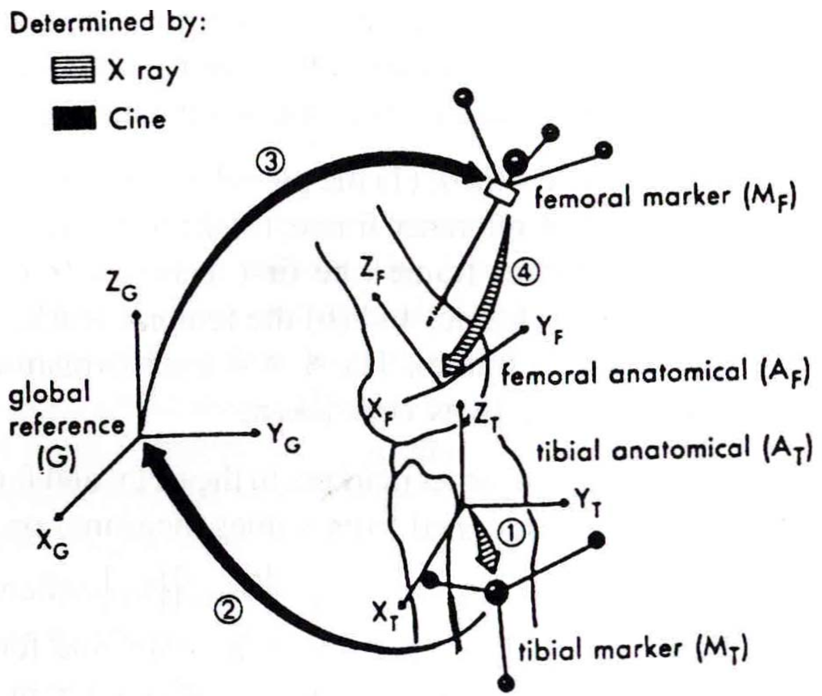

from *Journal of Biomechanics, 25,* Lafortune, M.A., et al, Three-dimensional kinematics of the human knee during walking, 347-357, 1992.

Errors in motion of ‘rigid’ body segments
- skin mounted vs. bone mounted markers

- The pattern of errors due to movement of skin mounted markers in relation to the bones are subject specific
- Therefore, general correction strategies are not trivial to make

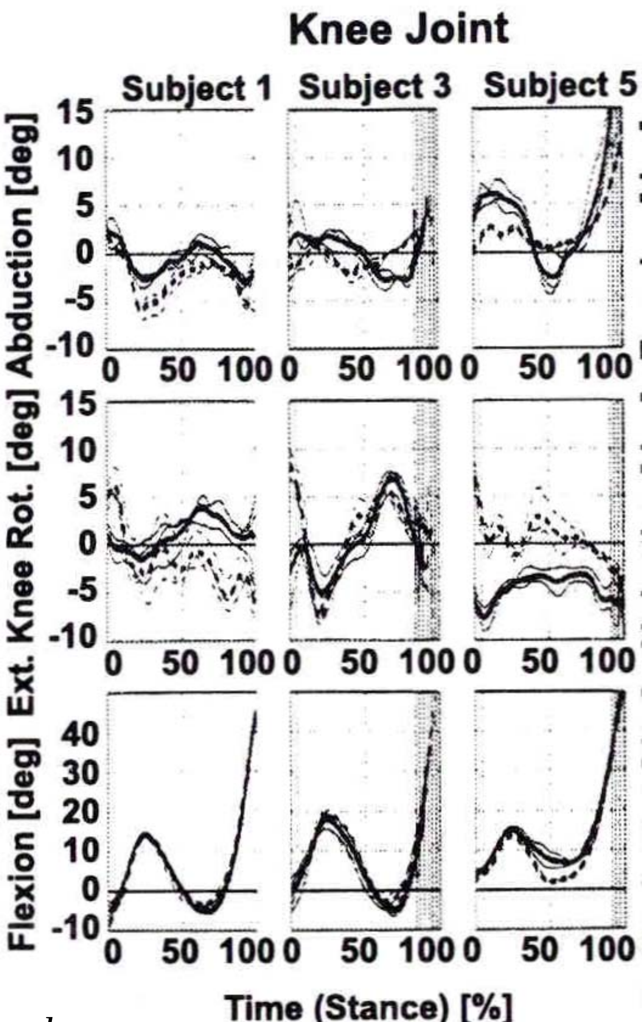

Solid line = bone mounted markers

Navicular bone axes of rotation

Bone mounted marker clusters
Reference recording - to establish the rotation matrix between the marker clusters and the bone coordinate systems

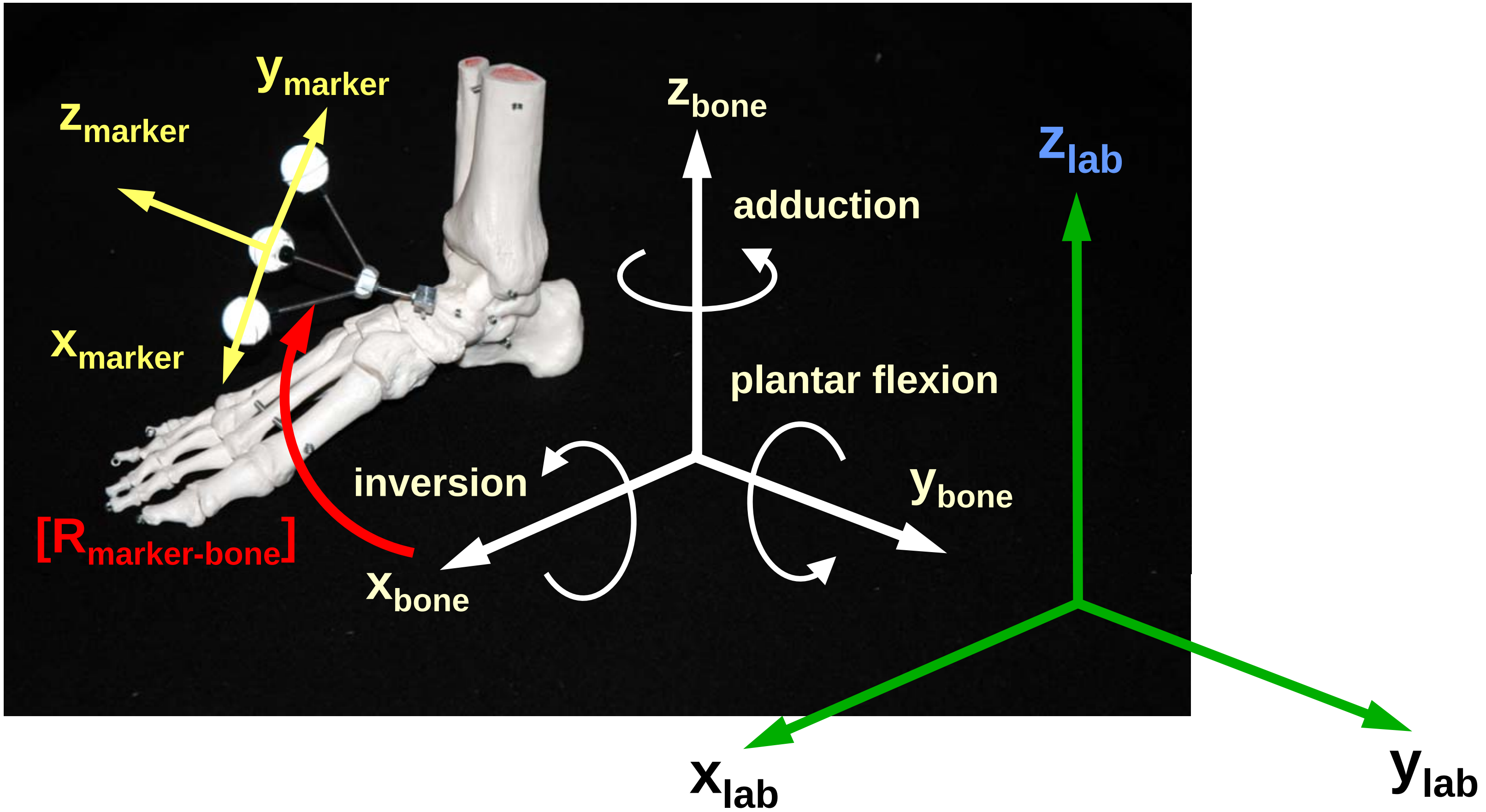

3D analysis of rearfoot and midfoot motion - bone mounted markers

- Description of rear foot (calcaneus) and midfoot (navicular) motion durig walking

- Evaluation of the acute effect on midfoot motion by application of orthotic insoles

Tibia

Calcaneus

Navicula

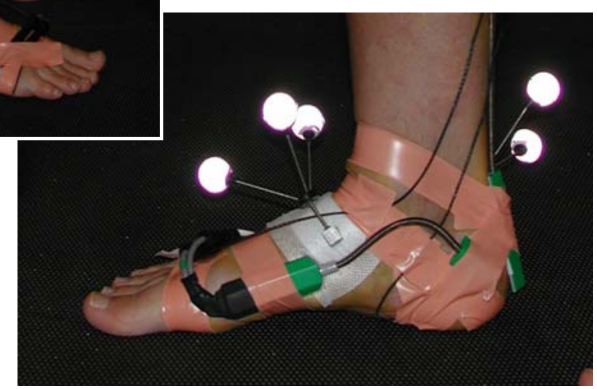

- 15 participants representing a wide range of medial arch heights (30 – 60 mm)

Voigt et al. XX ISB conference 2005

Rearfoot vs. midfoot motion
- bone mounted markers

Maximal supination – pronation movement

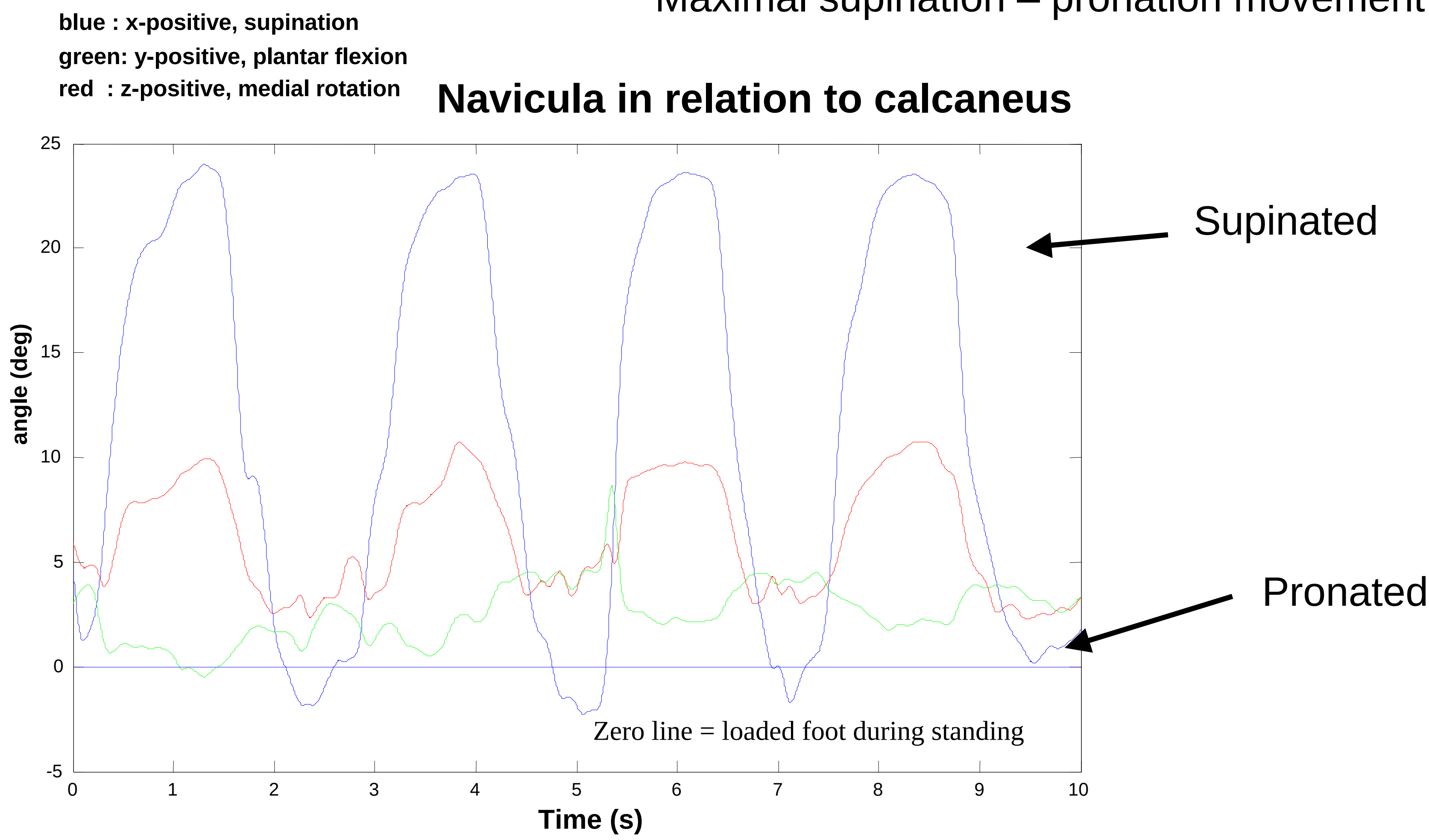

For clinical gait analysis

- different marker protocols can be used

Helen Hayes' Protocol (wands)

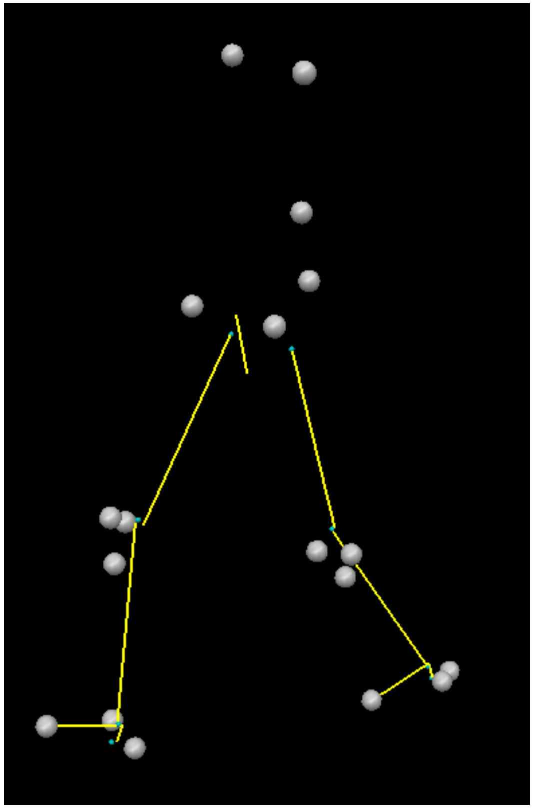

Lundbergs protocol

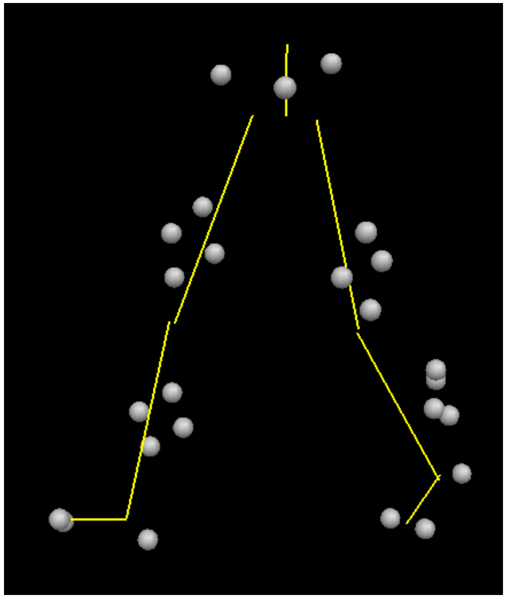

V3D Hybrid marker setup '6 DOF'

Kinetic information –

- measurement of forces

Marey's pneumatic analysis of human locomotion (from Centre National d'Art et de Culture Georges Pompidou, 1977, with permission of Ville de Beaune, Conservation des Musées).

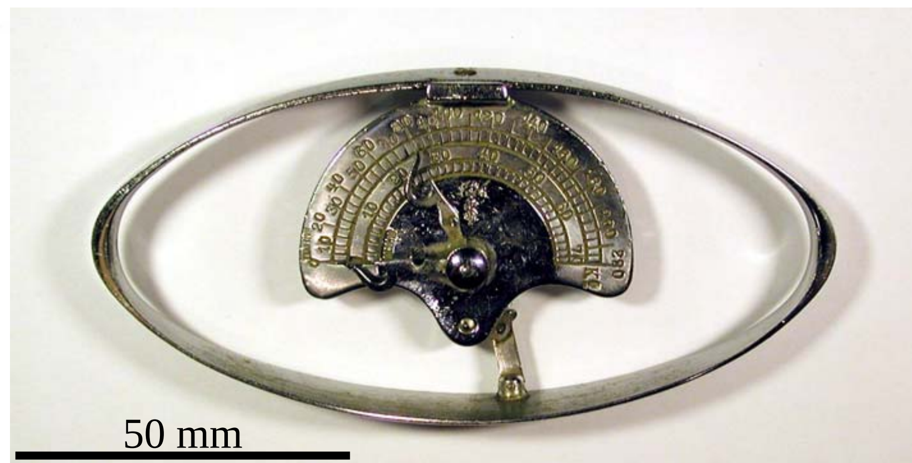

Force measurement principles

mechanical deformation of sensor ⇒ measurable electrical change ⇒ calibration to force

Electrical measurement principles :

- capacity
- conductivity
- change in electrical resistance
- piezoelectricity

Sensor types/materials :

div. types of capacitors
non-conducting di-electric material

div. types of conductors
conductive elastomers

strain-gauges
- foil strain gauges
- semiconductors
- mercury/saline

quarts crystals
('load washers')

Example applications :

measurement of pressure distribution (N/m^2)
biomechanics: shoes, seats, mattresses

force measurement, general (N, Nm)
div. types of force transducers in industry, science (tension, compression, shear and torsion)

biomechanical applications
- dynamometers for static and dynamic force measurements
- force plates
- tendon and ligament forces
- instrumented ergometers (e.g. bicycle,)

Strain gauge force measurement

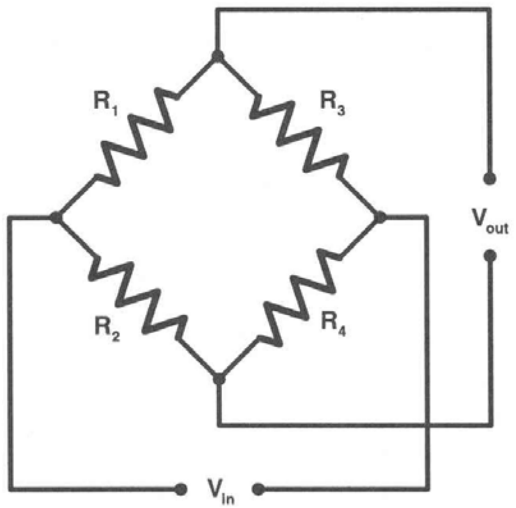

Wheatstone bridge circuitry for strain gauge operation.

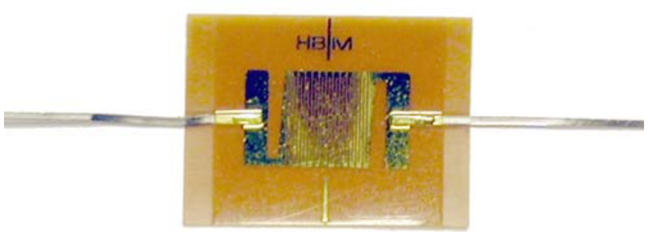

10 mm

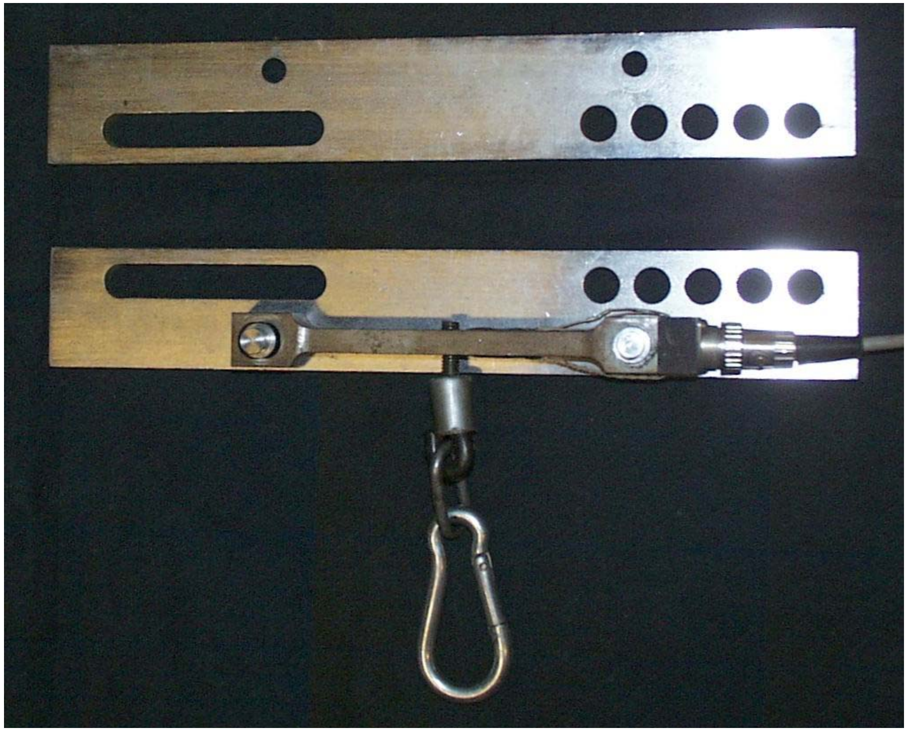

Piezoelectricity

- quartz (SiO_2), cut perpendicular to the crystallographic xy-axes

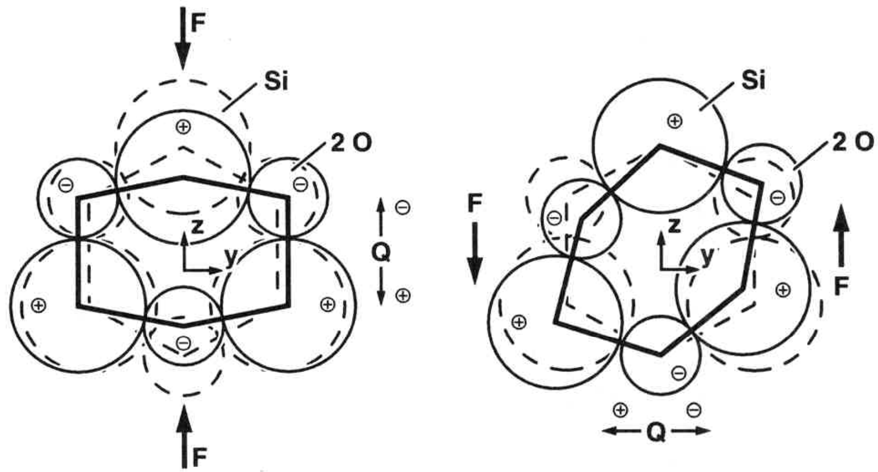

Schematic illustration of the piezoelectric effect (from Martini, 1983, with permission of the Instrument Society of America). Compressive forces produce a change in the electric charges on the surfaces where the force has been applied (left). Skew forces produce a change in charges on the surfaces perpendicular to the applied skew force direction (right).

- leakage
- preloading
- dynamic and quasi-static measurements

Application for gait analysis

- force plates
  - *reactive forces*
  - *reactive moments*
  - *derivation of point of force application ('COP')*

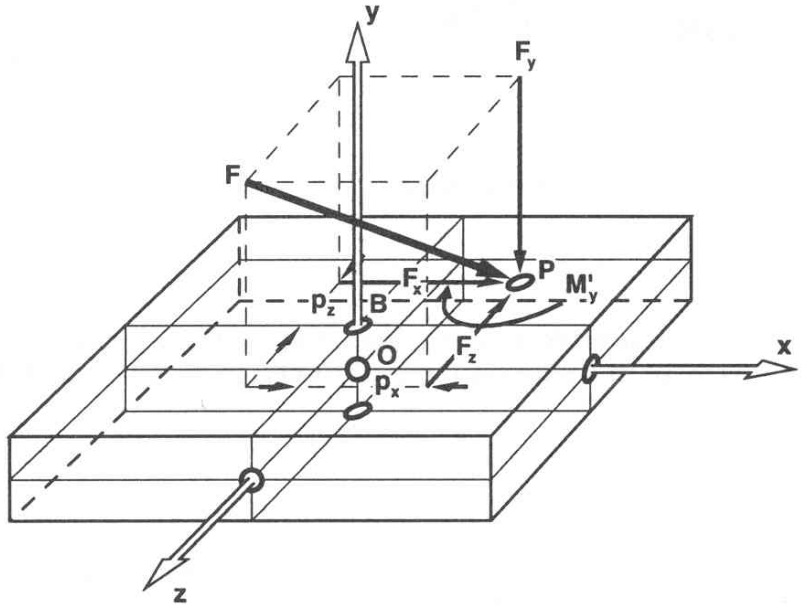

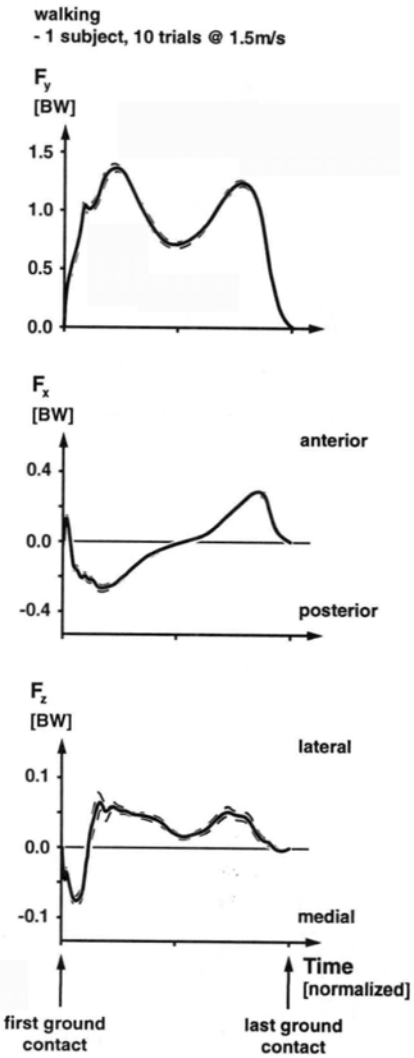

Calculating center of pressure (COP)
- point of application of the ground reaction vector (2D)

- calculation of center of pressure in the X-direction (e.g. sagittal plane)

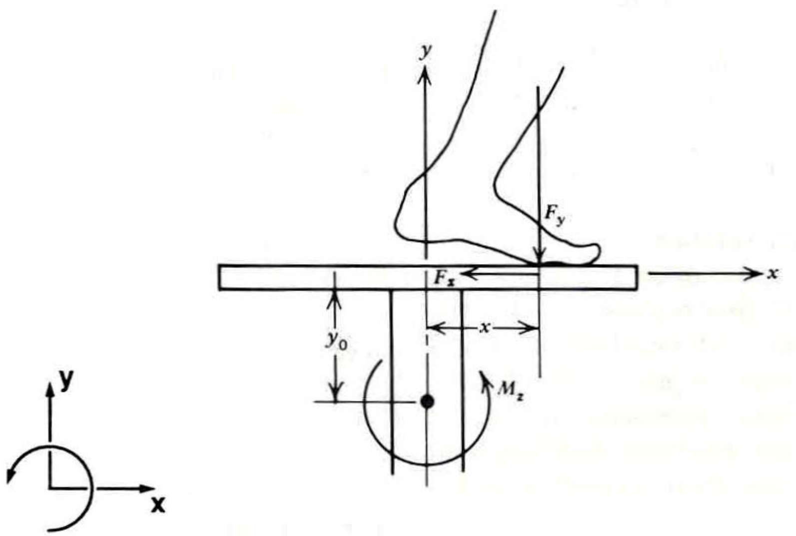

$$M_Z - F_Y \cdot x + F_X \cdot y_0 = 0$$

$$x = \frac{F_X \cdot y_0 + M_Z}{F_Y}$$

The force plate gives:

- F_x
- F_y
- M_z

y_0 = is specific to the construction of the given force plate and is provided by the factory

Similar calculation can be made for the frontal plane

Movement analysis

- Combining kinematic and kinetic information

  - inverse dynamics calculations

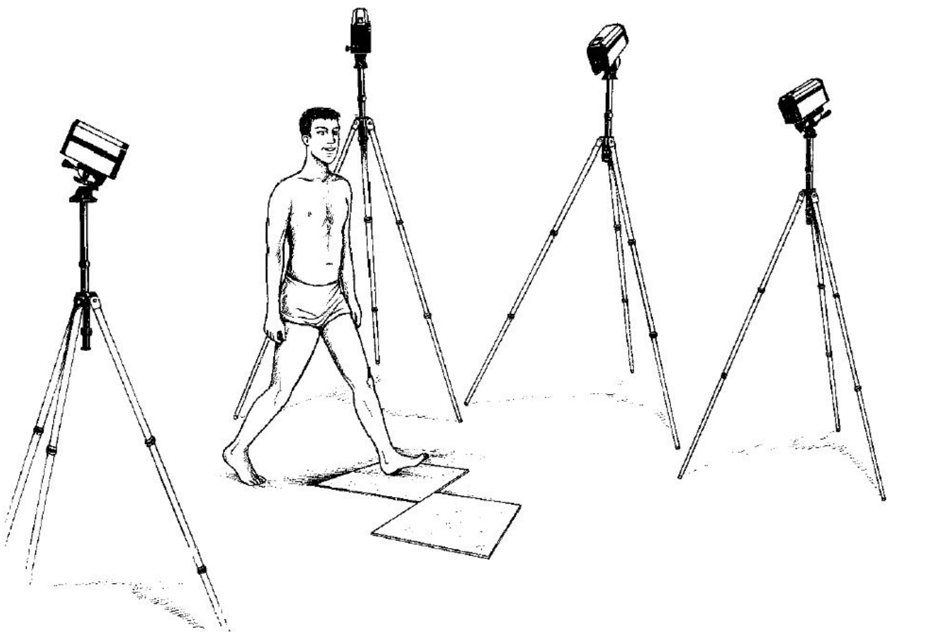

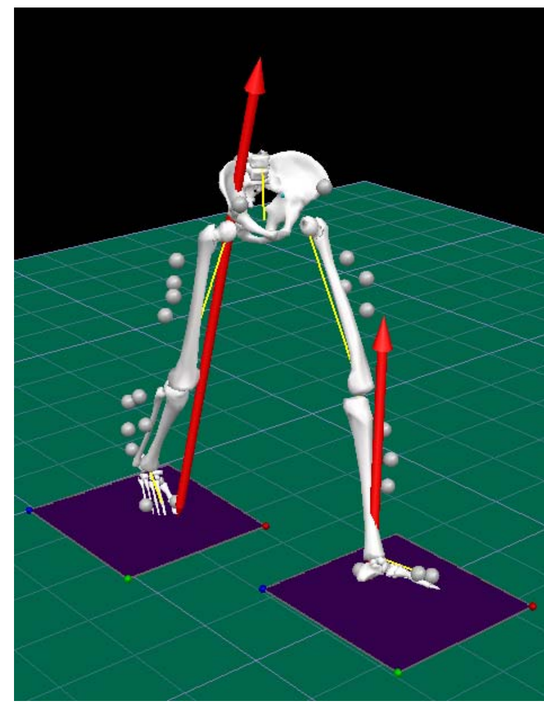

Combining kinematic and kinetic information
– coordinate systems

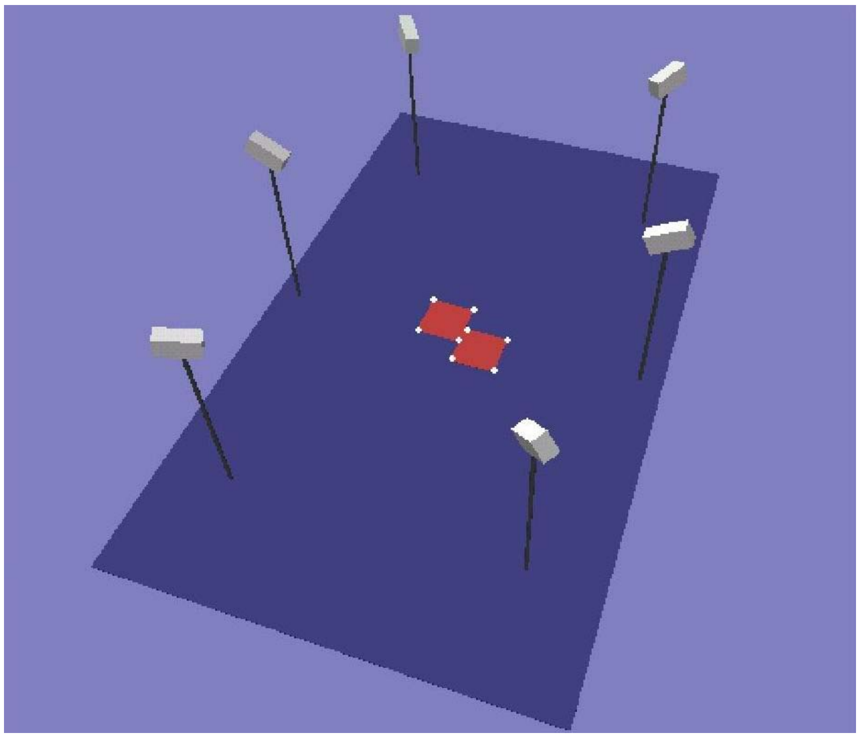

- force plates

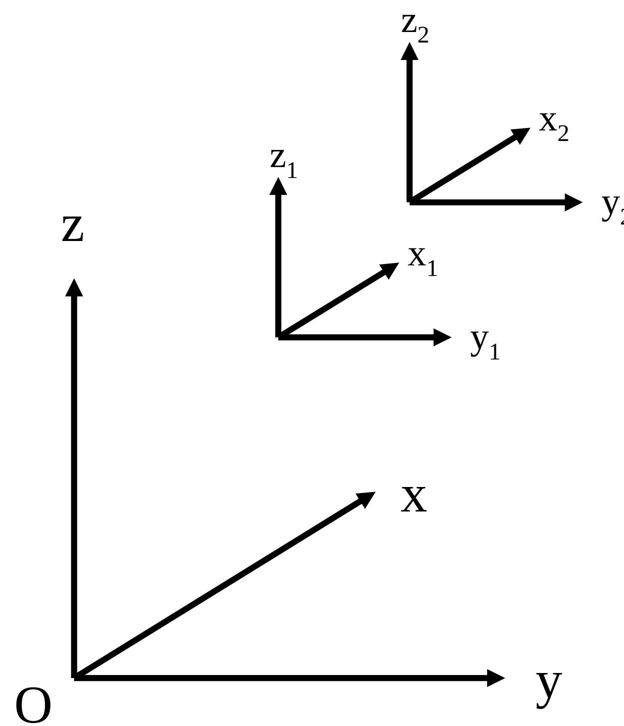

- global

Calculating center of pressure (COP)
- point of application of the ground reaction vector

- *a correct position of the COP is crucial in the calculation of net joint moments*

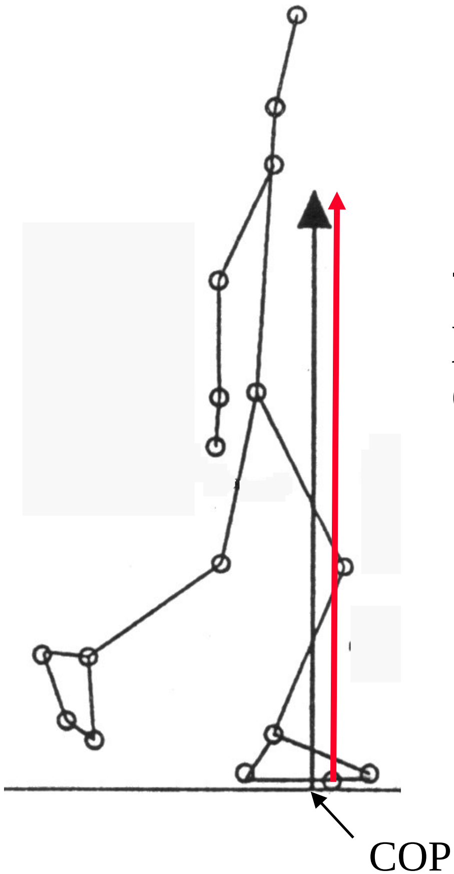

- e.g. if the 5th metatarsal marker position is used as the position of COP

Combining kinematic and kinetic information – inverse dynamic calculation

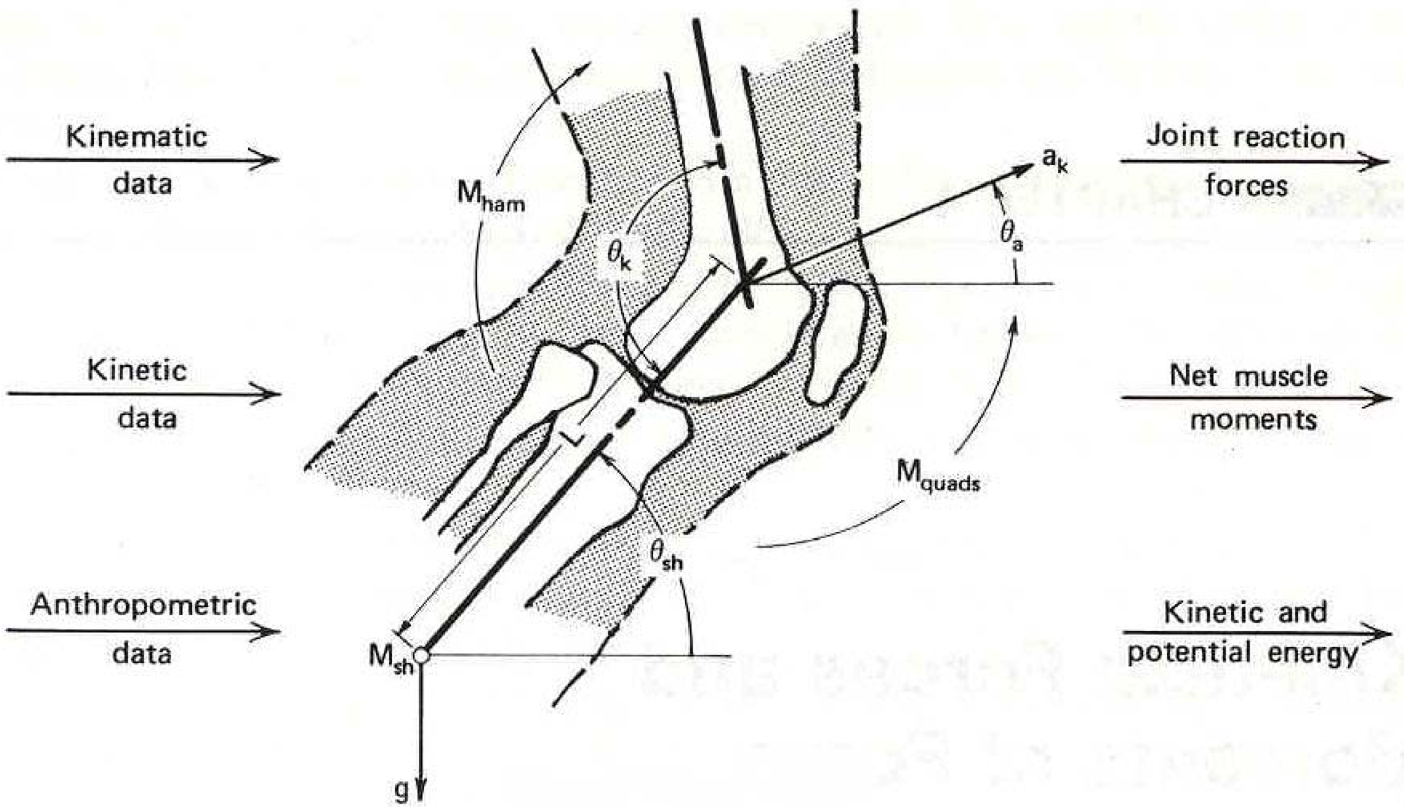

Combining kinematic and kinetic information

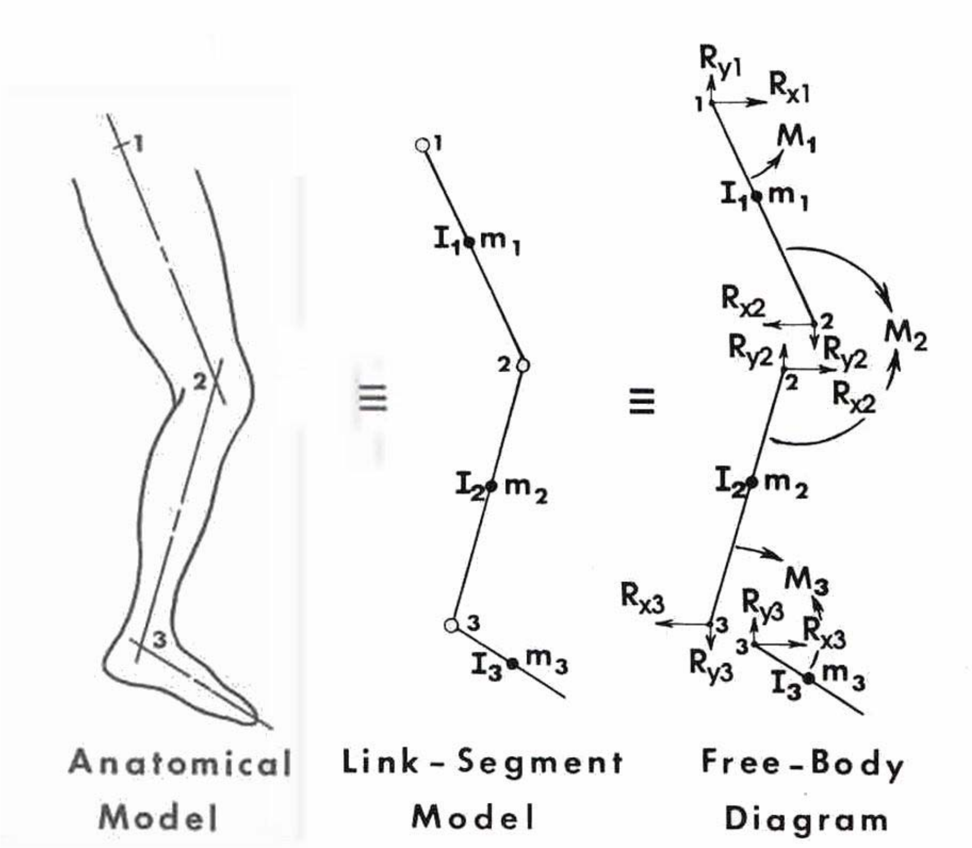

<u>Assumptions concerning the link segment model</u>

- each segment has a fixed mass located at its center of mass (which will be the center of gravity in vertical direction) i.e. a rigid body
- The location of each segments's center of mass remains fixed during the movement
- the joints are considered to be hinge (or ball and socket) joints
- The mass moment of inertia of each segment about its mass center (or about either the proximal or distal joints) is constant during the movement
- the length of the segment remains constant during the movement (e.g. the distance between hinge or ball and socket joints remains constant)

Anthropometric data

- segment weights, center of mass, radius of gyration

Table A.2 Anthropometric Data

SEGMENT	DEFINITION	SEG WEIGHT/ TOT BODY WT	CENTER OF MASS/ SEGMENT LENGTH PROX	DIST	RADIUS OF GYRATION/ SEGMENT LENGTH C of G	PROX	DIST	DENSITY
Hand	Wrist Axis/Knuckle II Middle Finger	.006 M	.506	.494 P	.297	.587	.577 M	1.16
Forearm	Elbow Axis/Ulnar Styloid	.016 M	.430	.570 P	.303	.526	.647 M	1.13
Upper Arm	Glenohumeral Axis/Elbow Axis	.028 M	.436	.564 P	.322	.542	.645 M	1.07
Forearm & Hand	Elbow Axis/Ulnar Styloid	.022 M	.682	.318 P	.468	.827	.565 P	1.14
Total Arm	Glenohumeral Joint/Ulnar Styloid	.050 M	.530	.470 P	.368	.645	.596 P	1.11
Foot	Lateral Malleolus/Head Metatarsal II	.0145 M	.50	.50 P	.475	.690	.690 P	1.10
Shank	Femoral Condyles/Medial Malleolus	.0465 M	.433	.567 P	.302	.528	.643 M	1.09
Thigh	Greater Trochanter/Femoral Condyles	.100 M	.433	.567 P	.323	.540	.653 M	1.05
Foot & Shank	Femoral Condyles/Medial Malleolus	.061 M	.606	.394 P	.416	.735	.572 P	1.09
Total Leg	Greater Trochanter/Medial Malleolus	.161 M	.447	.553 P	.326	.560	.650 P	1.06
Head & Neck	C7-T1 & 1st Rib/Ear Canal	.081 M	1.000	– PC	.495	1.116	– PC	1.11
Shoulder Mass	Sternoclavicular Joint/Glenohumeral Axis		.712	.288				1.04
Thorax	C7-T1/T12-L1 & Diaphragm*	.216 PC	.82	.18				0.92
Abdomen	T12-L1/L4-L5*	.139 LC	.44	.56				
Pelvis	L4-L5/Greater Trochanter*	.142 LC	.105	.895				
Thorax & Abdomen	C7-T1/L4-L5*	.355 LC	.63	.37				
Abdomen & Pelvis	T12-L1/Greater Trochanter*	.281 PC	.27	.73				1.01
Trunk	Greater Trochanter/Glenohumeral Joint*	.497 M	.50	.50				1.03
Trunk Head Neck	Greater Trochanter/Glenohumeral Joint*	.578 MC	.66	.34 P	.503	.830	.607 M	
H.A.T.	Greater Trochanter/Glenohumeral Joint*	.678 MC	.626	.374 PC	.496	.798	.621 PC	
H.A.T.	Greater Trochanter/Mid Rib	.678	1.142		.903	1.456		

* NOTE: These segments are presented relative to the length between the Greater Trochanter and the Glenohumeral Joint.

SOURCE CODES
- M - Dempster via Miller & Nelson
- P - Dempster via Plagenhoef
- L - Dempster via Plagenhoef from living subjects
- C - Calculated

NB! $I_0 = m\, p_0^2$

I_0 = moment of inertia, p_0 = radius of gyration, m = mass

Anthropometric data

- segment lengths

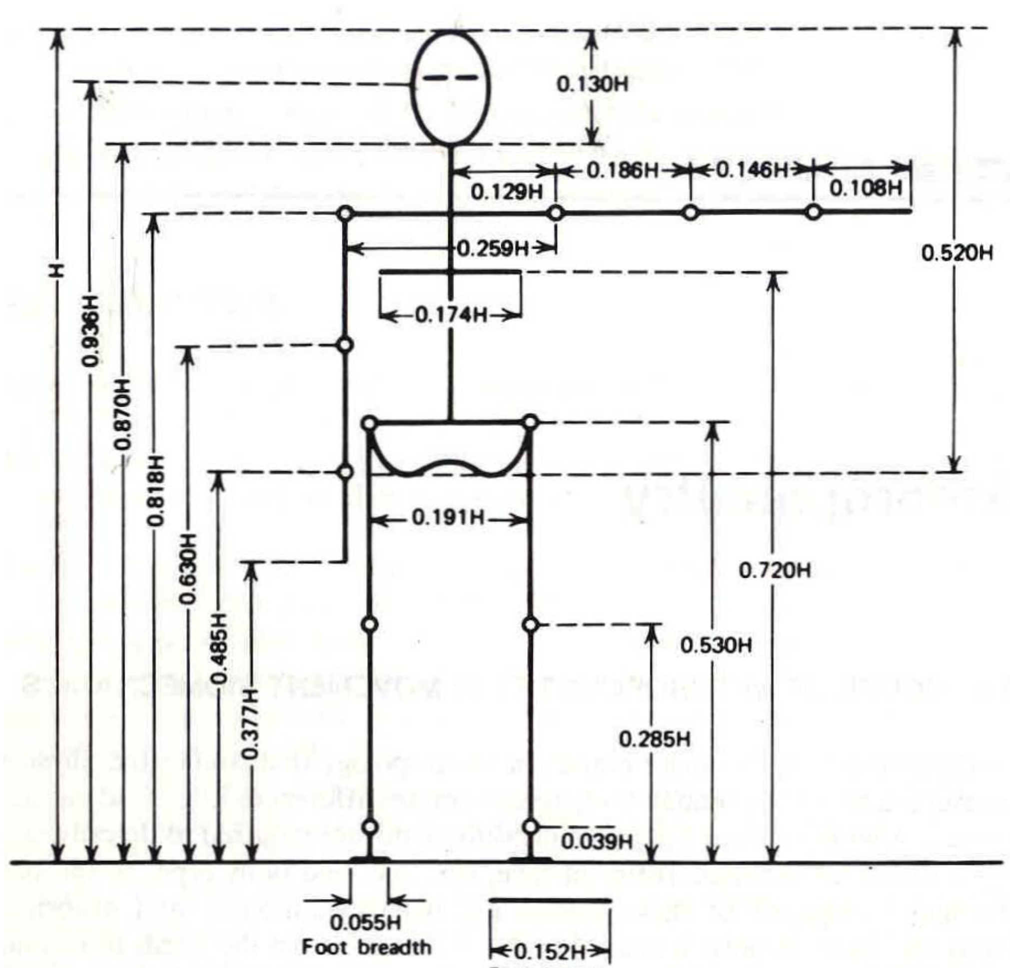

Equations of motion

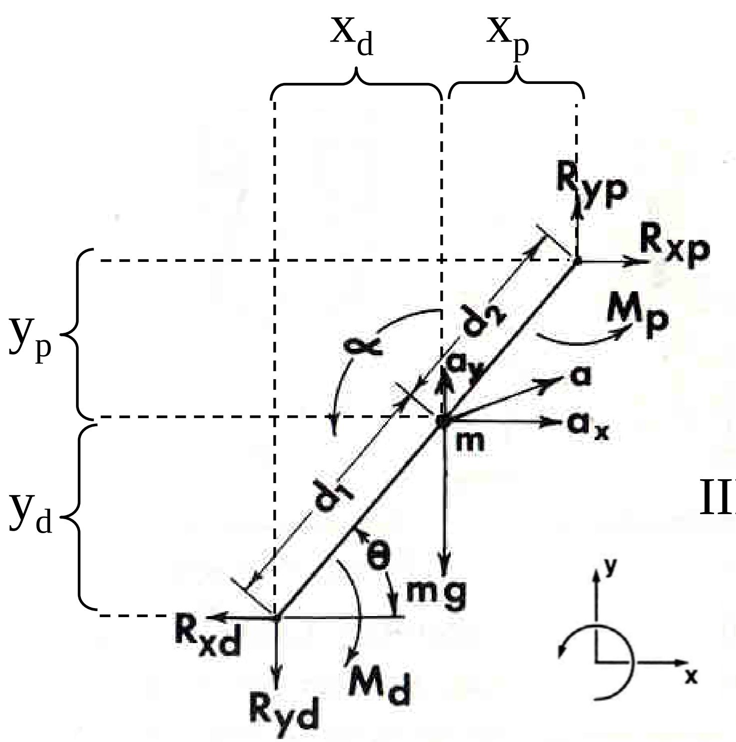

I. $\sum F_x = m\,a_x$

$R_{xp} - R_{xd} = m\,a_x$

II. $\sum F_y = m\,a_y$

$R_{yp} - R_{yd} - mg = m\,a_y$

III. $\sum M = I_O\,\alpha$

$M_p - M_d - R_{xd}\,y_d + R_{yd}\,x_d - Rx_p\,y_p + R_{yp}\,x_p = I_O\,\alpha$

- The calculation of forces and moments is initiated at a distal segment acting on the surroundings where the external reaction forces are measured e.g.
  - the foot during walking
  - the hands during pushing and pulling
- The unknowns are Mp and Rxp and Ryp
- Mp is the net joint (or muscle) moment

d = distal
p = proximal

Net joint moments (net muscle moments)
- the sum of the all muscle moments

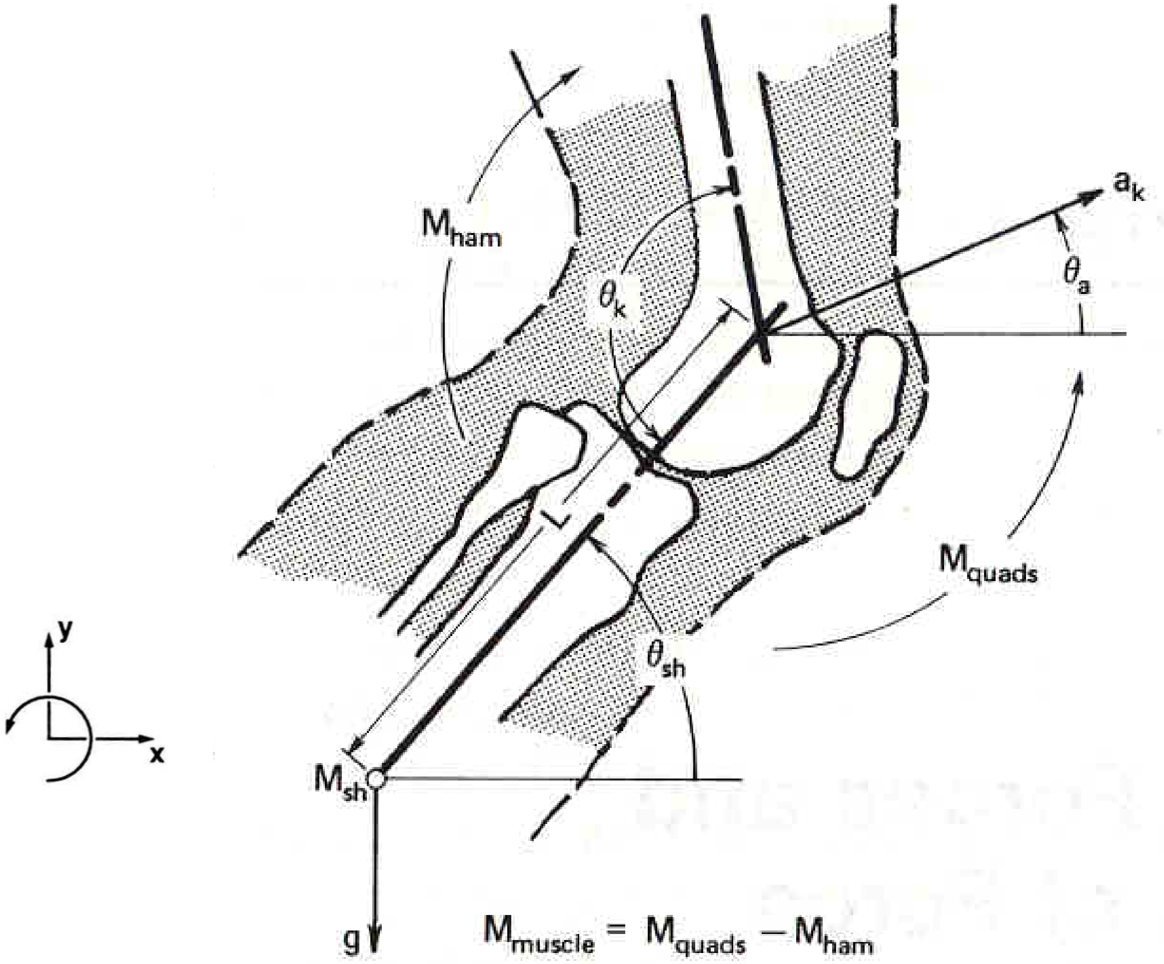

Net joint moments (net muscle moments)

- patient with total hip replacement
 3 consecutive trials

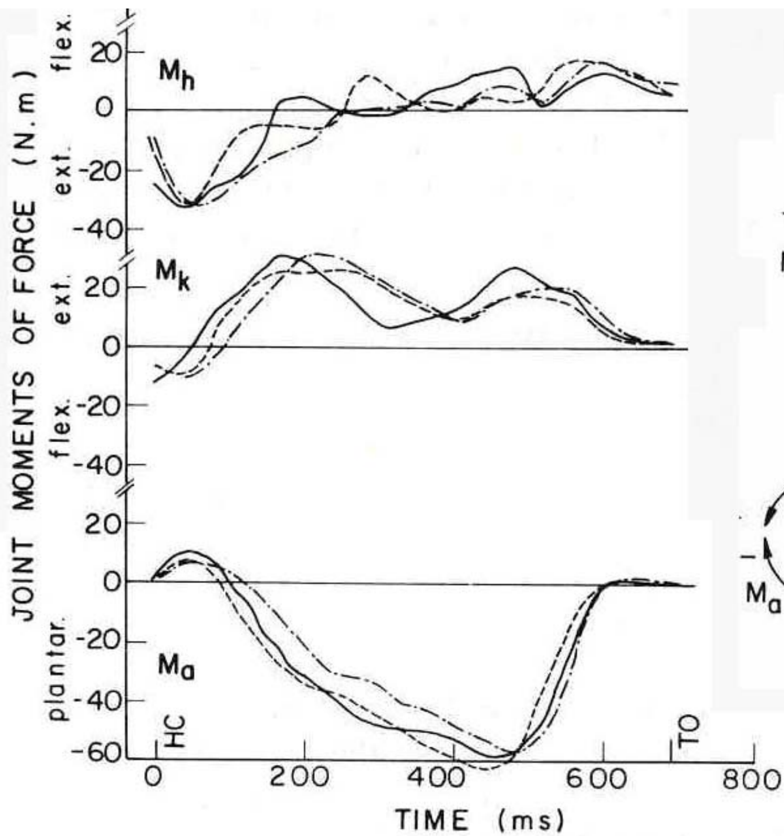

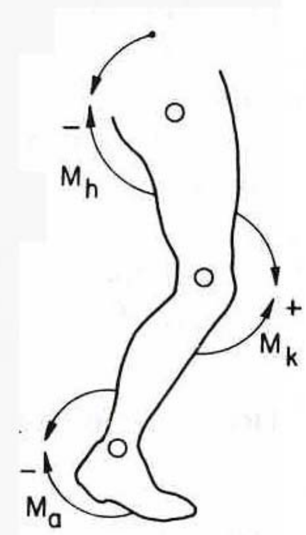

- counter clockwise is defined as positive

Consequently :

1. plantar flexing moment is negative
2. knee extension moment is positive
3. hip extension moment is negative

- how to determine the type of net muscle action (eccentric – concentric) ?

Joint moments and angular information
- to evaluate net muscle power and work

extension positive

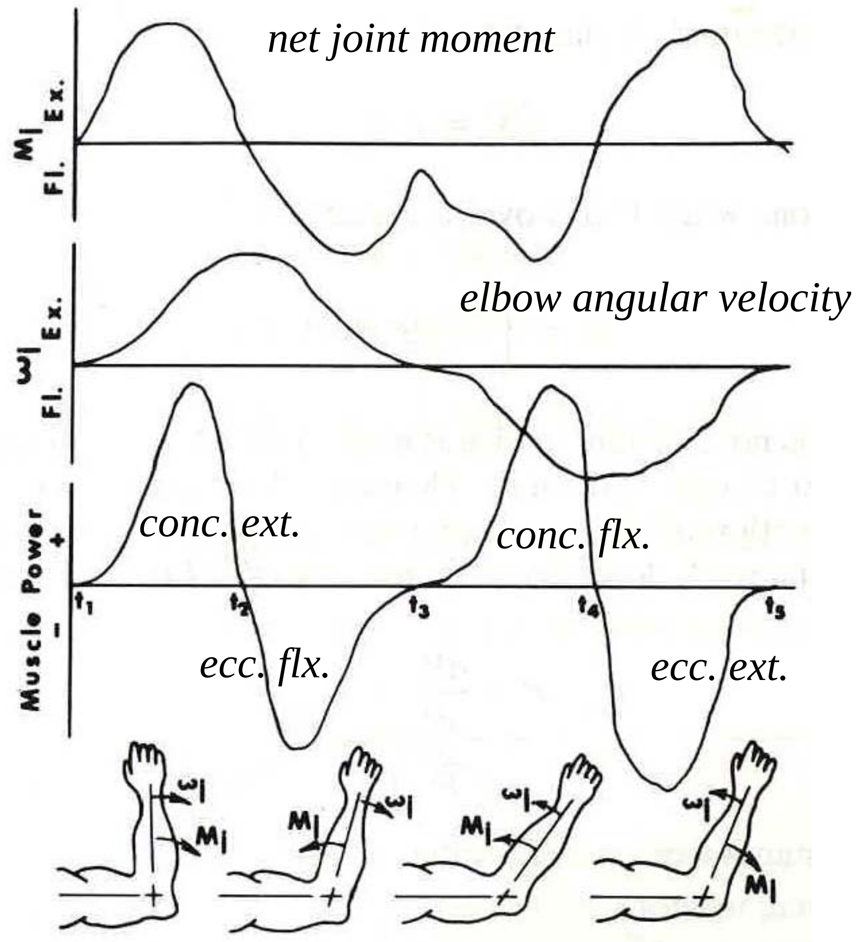

net joint power

$$P_m = M_j \omega_j \quad \mathrm{W}$$

where P_m = muscle power, watts

M_j = net muscle moment, N · m

ω_j = joint angular velocity, rad/s

net joint work

$$W_m = \int_{t_1}^{t_2} P_m \, dt \quad \mathrm{J}$$

Movement analysis
– biomechanical analysis of the effect of a drop foot stimulator

Neurostimulator KDC 2000A

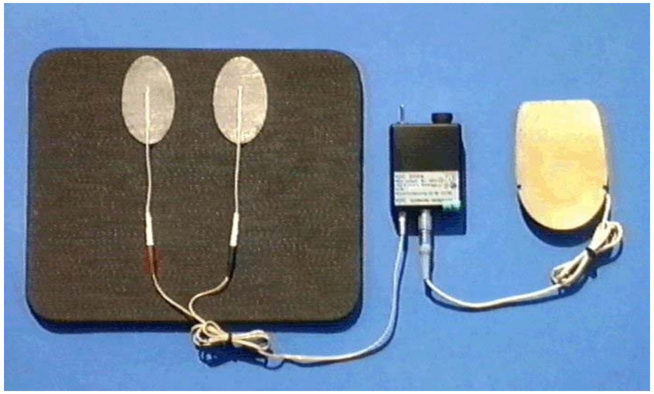

Stimulator function

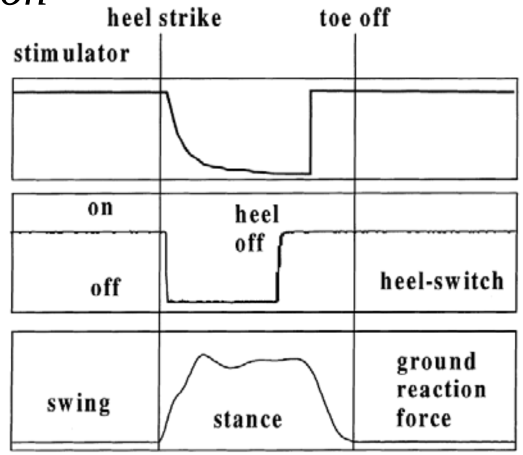

Voigt and Sinkjaer (2000) Clin Biomech 15: 340-351

Laboratory setup

– biomechanical analysis of the effect of a drop foot stimulator

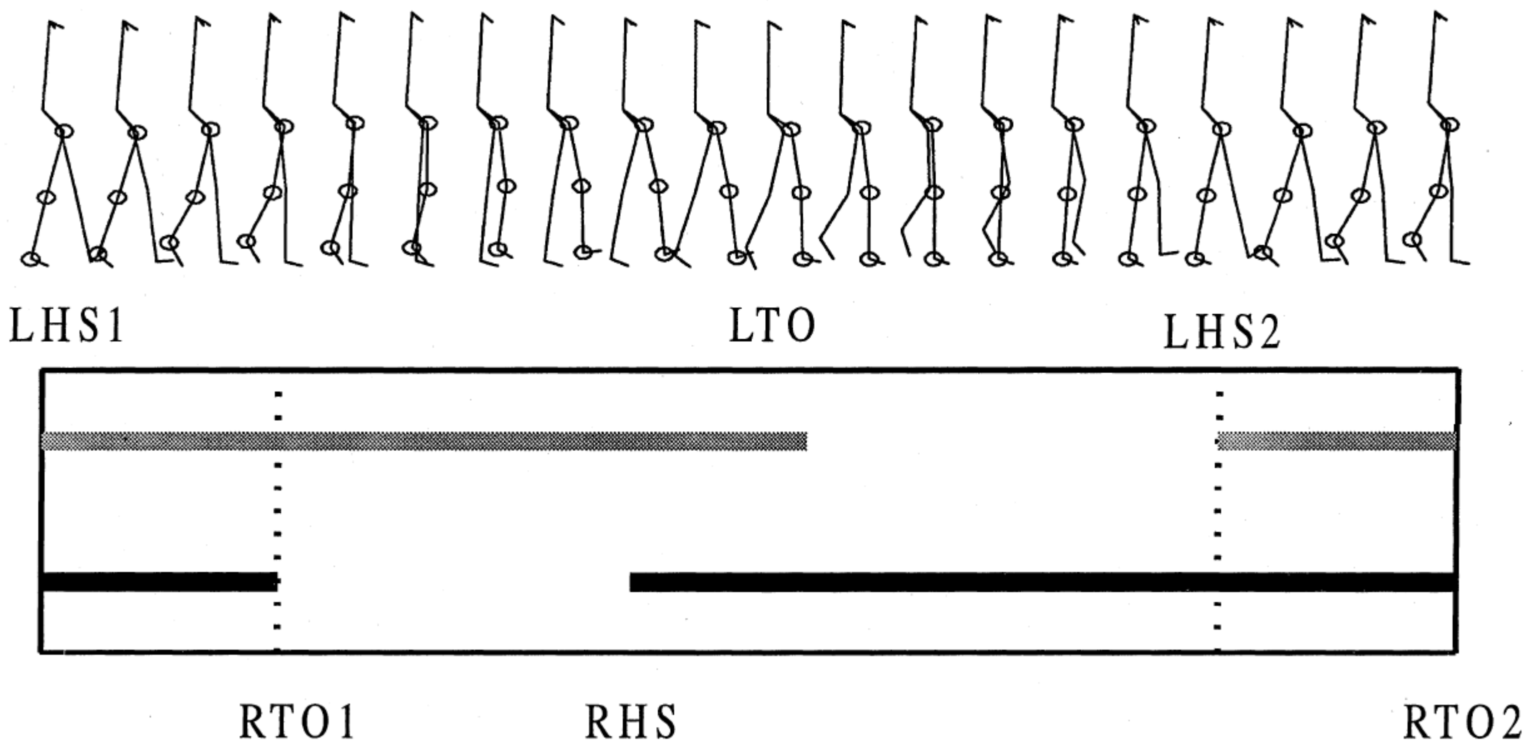

Gait parameters

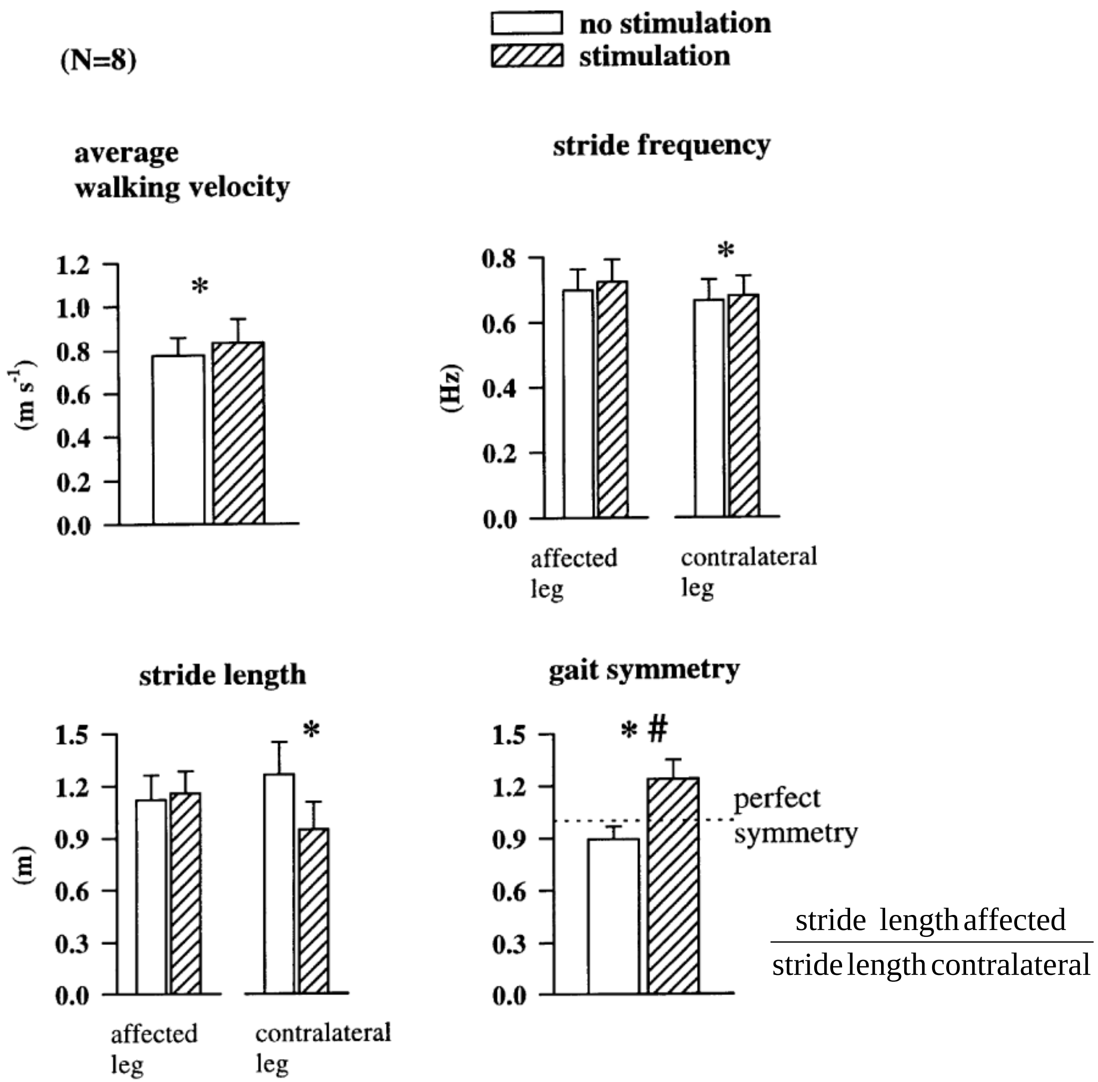

Joint moments and angular information

- to evaluate muscle action and net muscle work

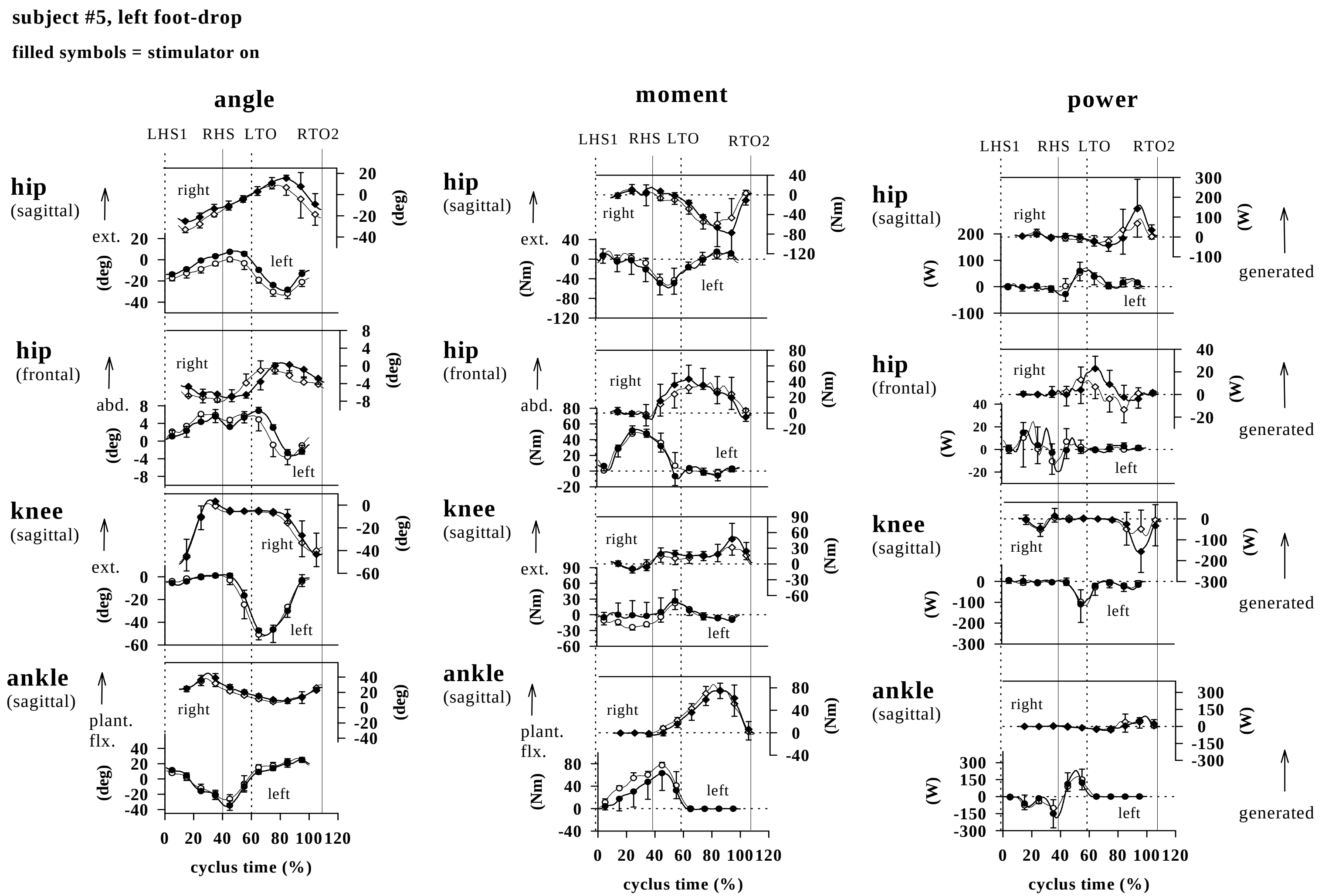

Joint powers

- evaluation of net muscle work in hemiplegic patients

NB!

At the hip
- H1-S (extensor generation) is missing at both sides
- H3-F (abductor generation) exaggerated on the contra-lateral side

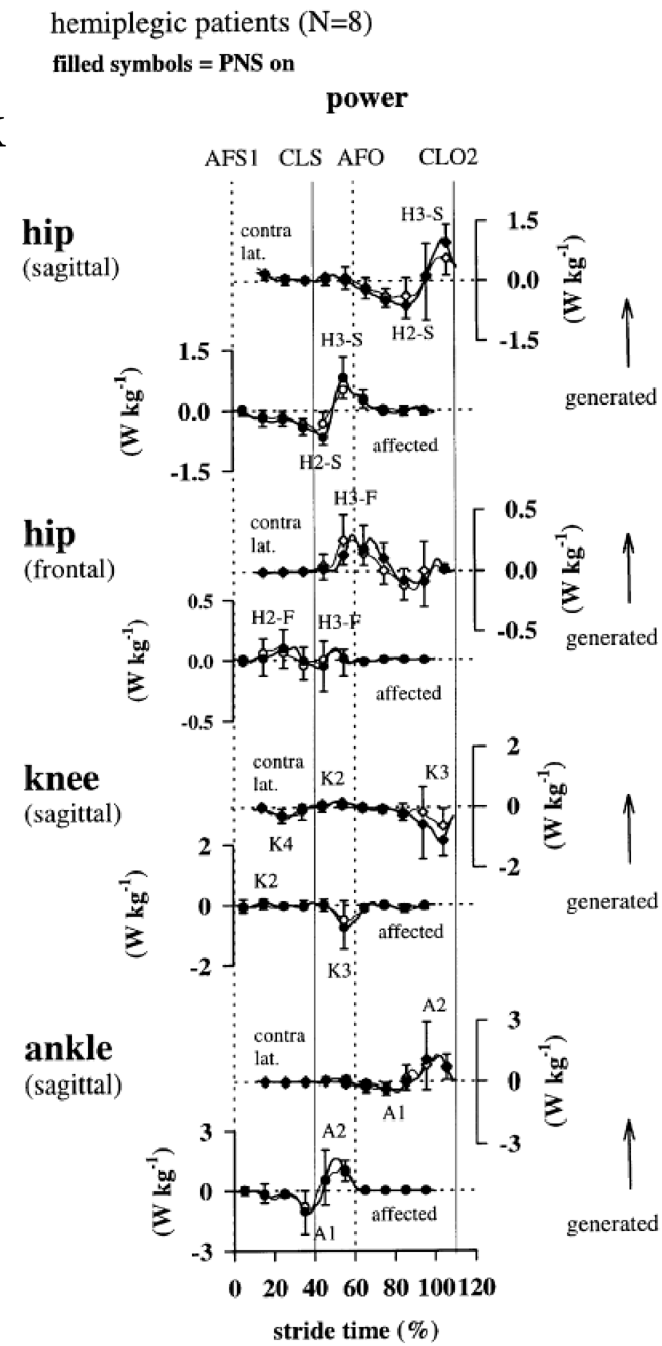

Efficiency/economy of movement

Clinical measure e.g. hemiplegic walking
-*walking efficiency determined as :*
the total positive work divided with the walking velocity

At preferred walking velocity:

Hemiplegic ($0.78\ ms^{-1}$): $\underline{2.75\ (J\ kg^{-1})*(m\ s^{-1})^{-1}}$
Normal ($1.60\ ms^{-1}$): $\underline{1.21\ (J\ kg^{-1})*(m\ s^{-1})^{-1}}$

Voigt and Sinkjaer (2000) Clin Biomech 15: 340-351

Gait characteristics in club-foot operated children - M. Cortsen, K. Christensen, M. Voigt

Ankle joint angle :
- shifted towards dorsiflexion

Prolonged stance time

CF children:
59.1, SD 1.6 % cyclus time
(p<0.05)

Healthy children:
57.8, SD 1.0% cyclus time

- Better control of Achilles tendon lengthening procedures!

Average profiles (N=13, unilateral)

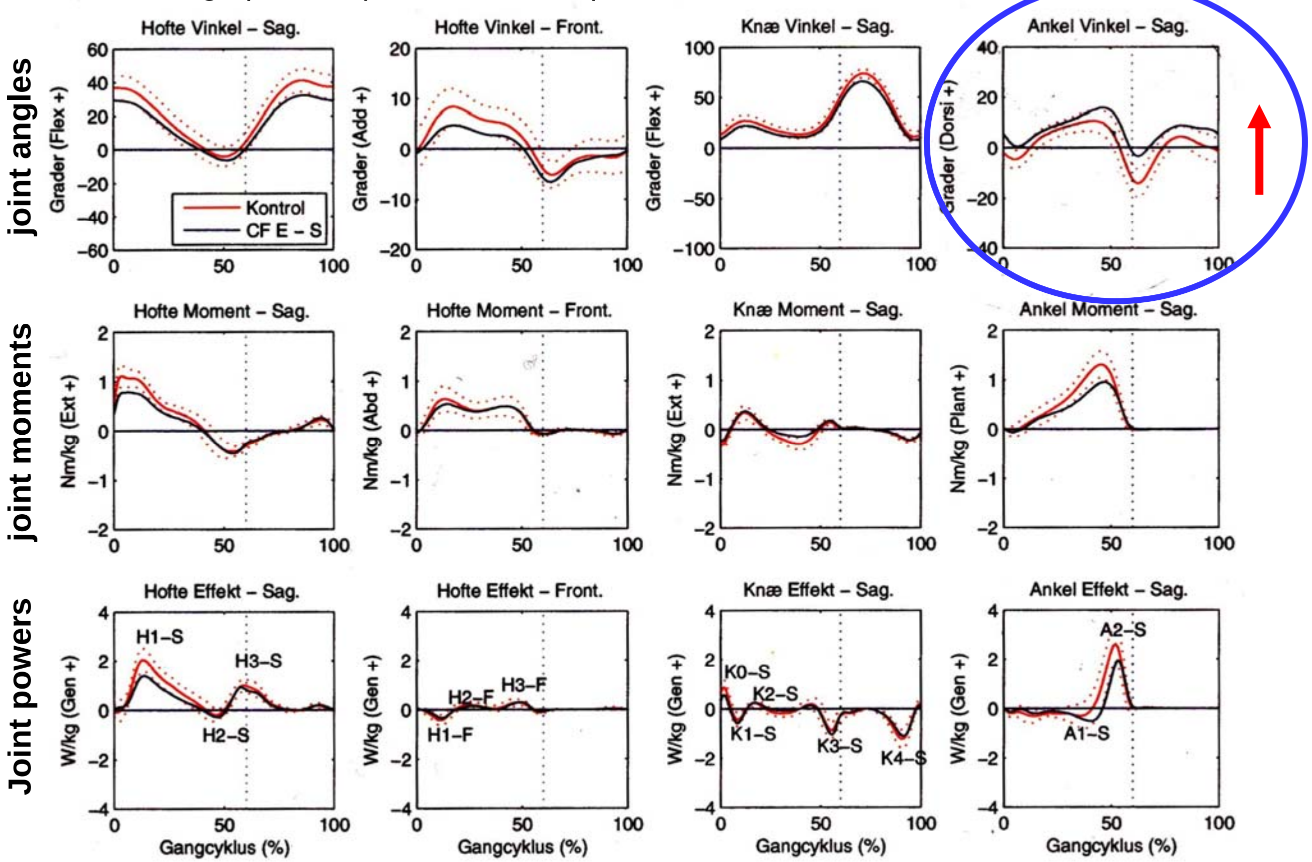

Direct measurement of in vivo tendon forces

- animal

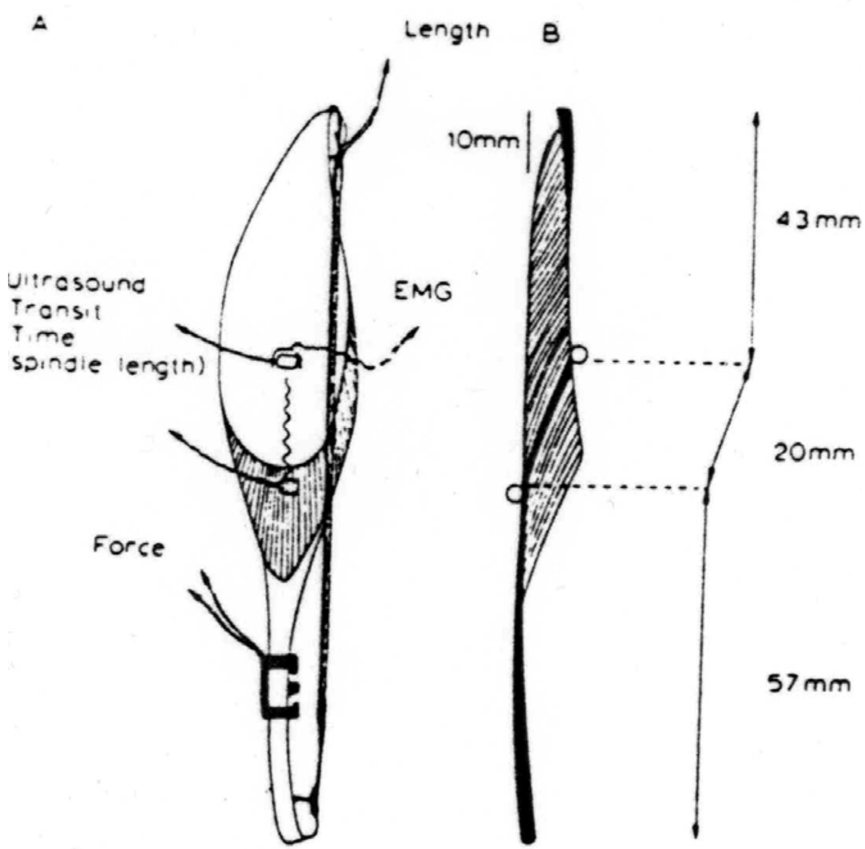

(from Hoffer et al. 1989)

Direct measurement of muscle-tendon behavior in vivo

- series elastic compliance – significance for motor control?

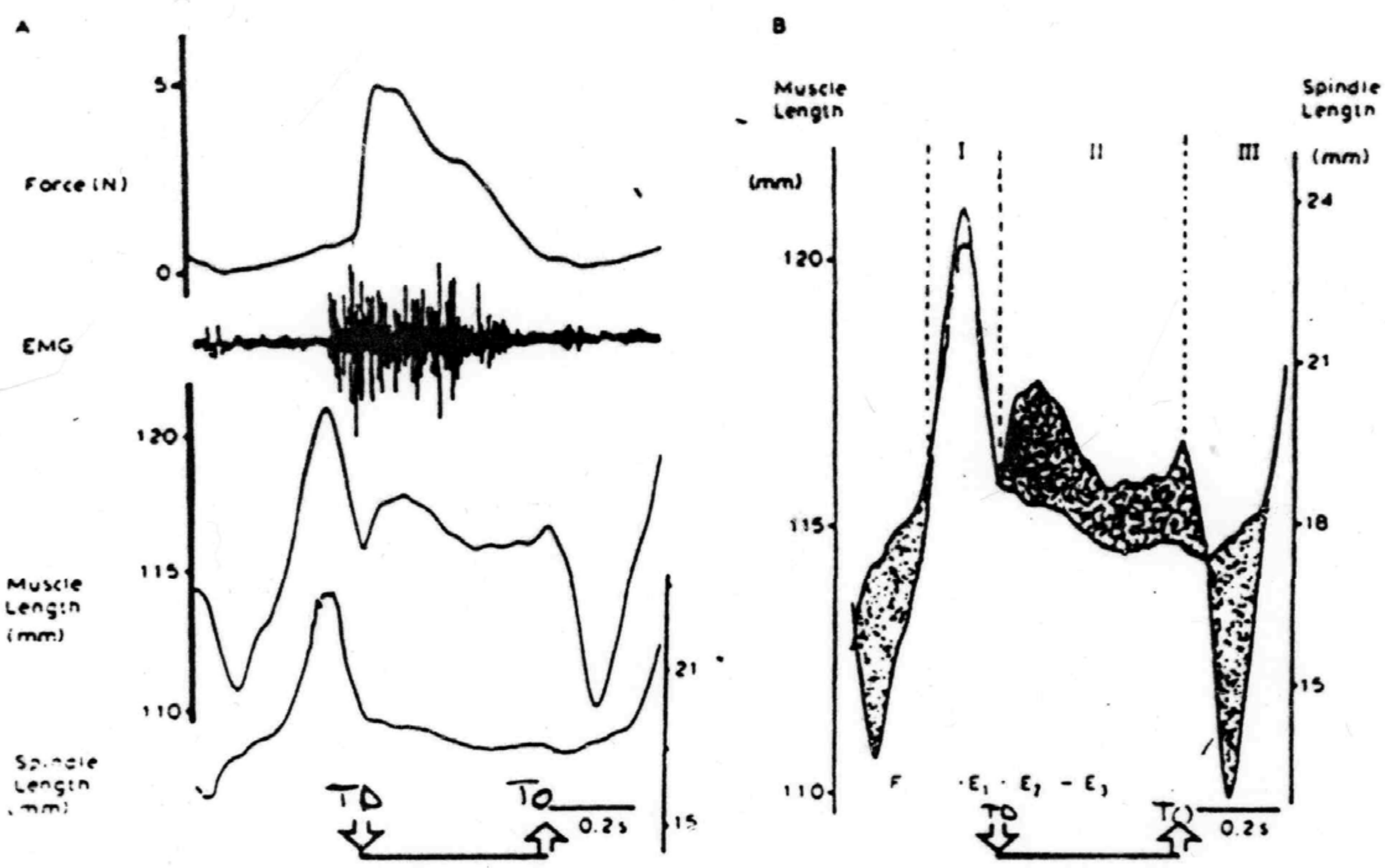

(from Hoffer et al. 1989)

Measurement of tendon forces in vivo
- in humans

buckle transducer

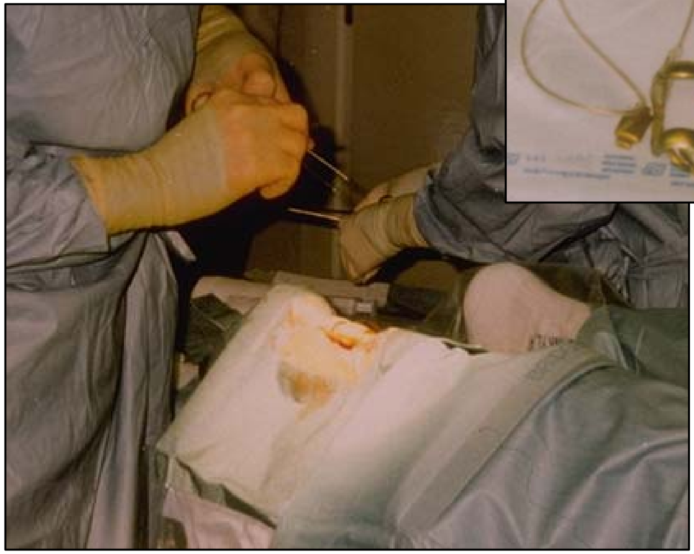

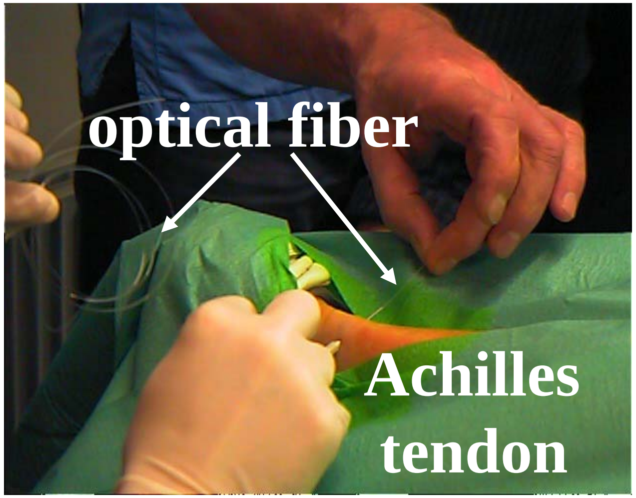

Calculation of muscle forces
-the force distribution problem

Indeterminate musculo-skeletal systems

The muscle force distribution is solved by means of :

- net joint moments is calculated (inverse dynamics)

- computer based musculo-skeletal models

- numerical techniques
  optimization

- Validation !!

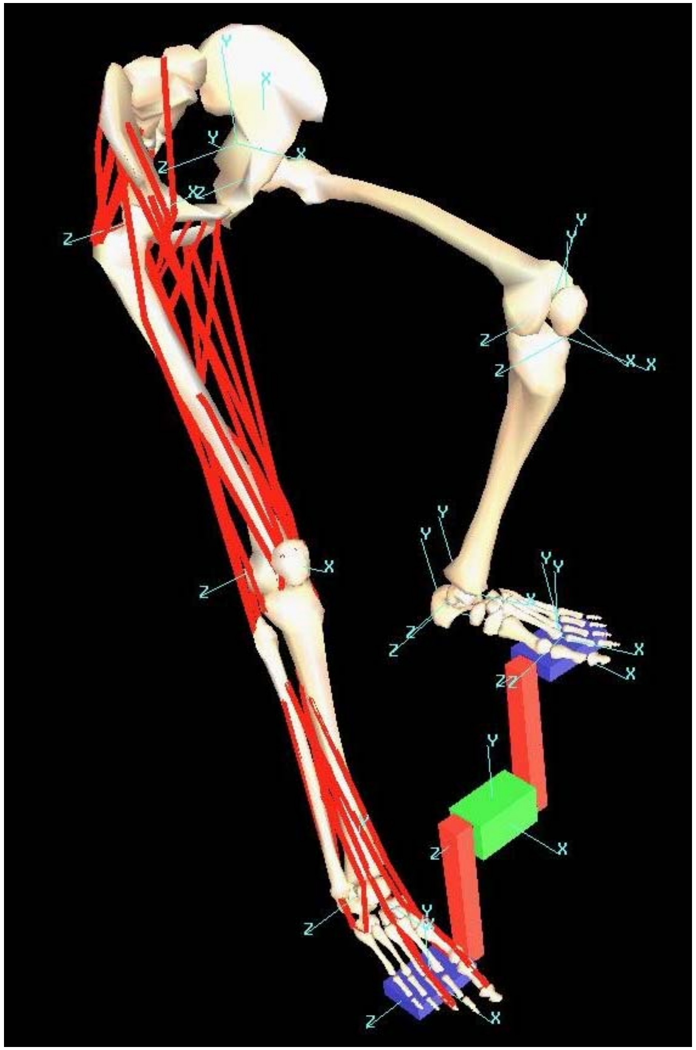

Calculation of muscle forces

- the force distribution problem

Technical note

Muscle recruitment by the min/max criterion — a comparative numerical study

John Rasmussen[a,*], Michael Damsgaard[a], Michael Voigt[b]

[a] Institute of Mechanical Engineering, Aalborg University, Pontoppidanstraede 101, 9220 Aalborg East, Denmark
[b] Center for Sensory-Motor Interaction, Aalborg University, Institute of Exercise and Sport Sciences, University of Copenhagen, Denmark

Journal of Biomechanics 34 (2001) 409–415

2.3. The min/max criterion

It is possible to show (but not well-known) that the solution to the load distribution problem with a polynomial objective function of increasing order converges to the solution obtained using a min/max objective function:

$$G(\mathbf{f}^{(M)}) = \max\left(\frac{f_i^{(M)}}{N_i}\right), \quad i = 1, \ldots, n^{(M)}. \qquad (8)$$

This criterion distributes the collaborative muscle forces in such a way that the maximum relative muscle force is as small as possible.

- can be solved by simple linear programming in a computational efficient way

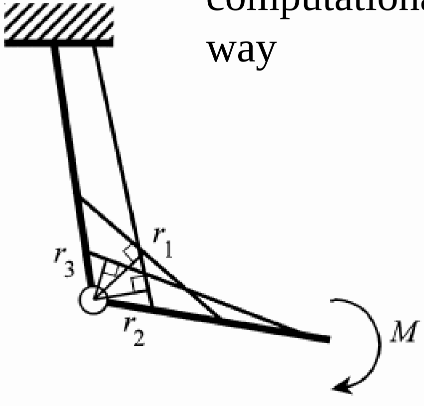

Fig. 1. Simple model of the dumbbell curl with the heavy lines designating the bones and the thin lines, the muscles. Muscles are numbered 1,2 and 3, and their effective moment arms are r_1, r_2, and r_3, respectively.

- Thank you for your attention